Role of aspartate 298 in mouse 5-HT_{3A} receptor gating and modulation by extracellular Ca^{2+}

Xiang-Qun Hu and David M. Lovinger

Laboratory for Integrative Neuroscience, National Institute on Alcohol Abuse and Alcoholism, National Institutes of Health, Bethesda, MD 20892-8115, USA

The TM2–TM3 extracellular loop is critical for activation of the Cys-loop family of ligand-gated ion channels. The contribution of aspartate 298 (D298), an amino acid that links the transmembrane domain 2 (TM2) to the TM2–TM3 loop, in mouse 5-hydroxytryptamine$_{3A}$ (5-HT_{3A}) receptor function was probed with site-directed mutagenesis in the present study. This negatively charged residue was replaced with an alanine to neutralize the charge, with a glutamate to conserve the charge, or with an arginine to reverse the charge. Human embryonic kidney 293 (HEK 293) cells transfected with the wild-type and mutant receptors were studied by combining whole-cell patch-clamp recording with fast agonist application. The D⟶A or D⟶R mutations resulted in a receptor with reduced 5-HT potency, and accelerated kinetics of desensitization and deactivation. In addition, the efficacy of partial agonists was reduced by the D⟶A mutation. The D⟶E mutation produced a receptor with properties similar to those of the wild-type receptor. In addition, the potential role of this residue in modulation of the receptor by extracellular calcium ($[Ca^{2+}]_o$) was investigated. Increasing $[Ca^{2+}]_o$ inhibited 5-HT-activated currents and altered receptor kinetics in a similar manner in the wild-type and D298E receptors, and this alteration was eliminated by the D⟶A and D⟶R mutations. Our data suggest that the charge at D298 participates in transitions between functional states of the 5-HT_{3A} receptor, and provide evidence that the charge of the side-chain at residue D298 contributes to channel gating kinetics and is crucial for Ca^{2+} modulation.

(Received 20 June 2005; accepted after revision 5 August 2005; first published online 11 August 2005)
Corresponding author D. M. Lovinger: Laboratory for Integrative Neuroscience, National Institute on Alcohol Abuse and Alcoholism, National Institutes of Health, 5625 Fishers Lane, Room TS-13A, Bethesda, MD 20852, USA. Email: lovindav@mail.nih.gov

The 5-hydroxytryptamine$_3$ (5-HT_3) receptor is a member of the Cys-loop ligand-gated ion channel superfamily, which includes nicotinic acetylcholine (nACh), γ-aminobutyric acid type A ($GABA_A$), glycine receptors, and a newly discovered Zn^{2+}-activated channel (Ortells & Lunt, 1995; Karlin, 2002; Reeves & Lummis, 2002; Davies *et al.* 2003). Whereas nACh and 5-HT_3 receptors are cationic channels, $GABA_A$ and glycine receptors are anionic channels. Receptors in this superfamily are comprised of a pentameric arrangement of subunits surrounding a central ion-conducting pore. Each subunit shares a common topology containing a large extracellular N-terminal domain, four transmembrane domains (TM1–TM4) and two short loops that link TM1 to TM2 and TM2 to TM3 (Fig. 1*A*). The neurotransmitter binding site lies in the extracellular N-terminal domain at the interface between subunits, whereas the channel pore is believed to be formed by TM2.

Binding of neurotransmitter to a ligand-gated ion channel triggers a complex conformational change which ultimately results in the opening and desensitization of the channel (Miyazawa *et al.* 2003). Several regions of these receptors are implicated in the coupling process between agonist binding and channel gating. For example, the TM1–TM2 loop of the glycine receptor (Lynch *et al.* 1997), and the pre-TM1 region of the 5-HT_{3A} (Hu *et al.* 2003) and glycine (Castaldo *et al.* 2004) receptors have been found to be involved in linking agonist binding to receptor activation.

The TM2–TM3 loop in the nACh, glycine and $GABA_A$ receptors also contributes to the coupling of binding and channel gating (Campos-Caro *et al.* 1996; Lynch *et al.* 1997; Rovira *et al.* 1998, 1999; Grosman *et al.* 2000; O'Shea & Harrison, 2000). In the 5-HT_{3A} receptor the only charged amino acid residue in the TM2–TM3 loop is aspartate 298 (D298) (Fig. 1*B*). This residue is analogous to the 20′ residue in the TM2 numbering system developed for

 DOI: 10.1113/jphysiol.2005.092866

the nACh receptor. We will refer to the D298 as part of the TM2–TM3 loop, but it should be noted that this residue may be part of the extended TM2 alpha-helical structure. The charge of this residue varies systematically among many members of the Cys-loop ligand-gated ion channels: negative for the cation-permeable subfamily (nACh and 5-HT_3 receptors) and positive for the anion-permeable subfamily ($GABA_A$ and glycine receptors). The analogous residue in the nACh receptors has been suggested to contribute to the attraction of permeating cations into the pore (Imoto *et al.* 1988). This residue may also play a role in channel gating (Lynch *et al.* 1997; O'Shea & Harrison, 2000). However, the generality of these findings to the whole receptor superfamily has not been examined. In the present study, we replaced the D298 residue with alanine, glutamate or arginine residues to alter amino acid side-chain charge. The contribution of D298 to 5-HT_{3A} receptor function was then examined in HEK 293 cells using whole-cell patch-clamp recording and fast solution application. Mutations at this residue to alanine or arginine reduced the sensitivity of the receptor to 5-HT, reduced the efficacy of partial agonists, and substantially accelerated channel gating kinetics. Substitution of glutamate at this residue largely preserved the wild-type receptor sensitivity to 5-HT and slightly decreased the kinetics of activation, desensitization and deactivation. Increasing extracellular Ca^{2+} ($[Ca^{2+}]_o$) inhibits wild-type receptor function and accelerates the kinetics of activation, desensitization and deactivation. These effects of $[Ca^{2+}]_o$ were abolished by the D→A or D→R mutations, but retained in the D→E mutation. These results indicate that the negative charge at D298 contributes to receptor-channel gating and is a critical determinant of the actions of Ca^{2+} on the 5-HT_{3A} receptor.

Methods

Mutagenesis

Point mutation of the mouse 5-HT_{3A} receptor (5-$HT_{3A(a)}$, long form, gift from Dr D. Julius, San Francisco, CA) was accomplished using a QuikChange site-directed mutagenesis kit (Stratagene, La Jolla, CA, USA). The successful incorporation of mutations was verified by sequencing the clones using an ABI Prism 377 automated DNA sequencer (Applied Biosystems, Foster

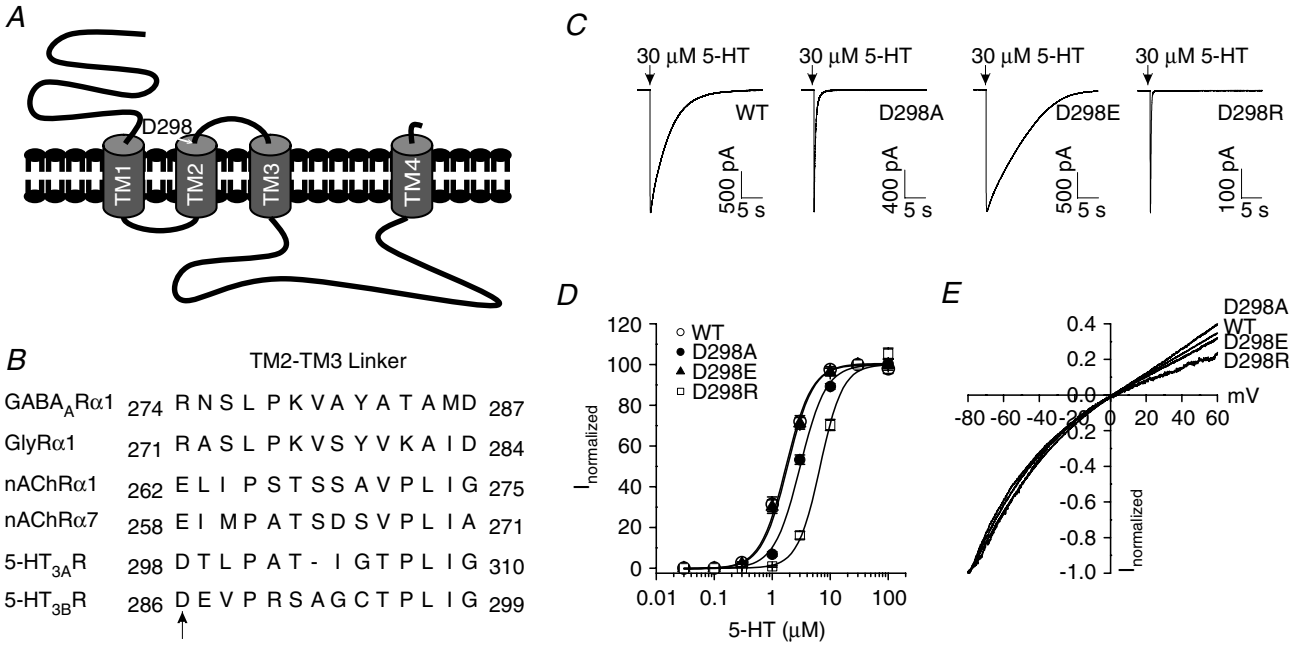

Figure 1. Position of D298 and effects of the D298 mutations on 5-HT concentration–response and *I–V* relationships

A, putative topology of the 5-HT_{3A} receptor. The arrow indicates the position of D298. *B*, sequence alignment of the TM2–TM3 loop from the Cys-loop ligand-gated ion channels. Arrow indicates the site of mutations. *C*, traces show current activated by 30 μM 5-HT from individual HEK 293 cells expressing the wild-type (WT) and mutant receptors. Arrows indicate the application of agonist. *D*, concentration–response curves of 5-HT-activated currents for the WT and mutant receptors. Data were normalized to peak current activated by 30 μM 5-HT for each cell. Each data point represents mean ± S.E.M. from 5 to 23 cells. Note the overlapping of curves for the WT and D298E receptors. *E*, voltage ramps obtained at the peak of current activated by 3 μM 5-HT. Currents activated by the voltage protocol in the absence of 5-HT have been subtracted. Data are normalized to the current amplitude obtained at −80 mV. Similar results were obtained from 5 to 7 cells.

City, CA, USA). The cDNAs were then subcloned into the vector pcDNA3.1 (Invitrogen Co., Carlsbad, CA, USA) for expression in human embryonic kidney (HEK) 293 cells (passage 12).

Cell culture and transient receptor expression

HEK 293 cells (American Type Culture Collection, Manassas, VA, USA) were grown in minimum essential medium (MEM, Invitrogen) supplemented with 10% horse serum, and maintained in a humidified incubator at 37°C in 5% CO_2. HEK 293 cells were transiently transfected with the wild-type or mutant 5-HT_{3A} receptor cDNA using the Lipofectamine 2000 reagent (Invitrogen) according to the manufacturer's instructions. Green fluorescent protein (pGreen Lantern, Invitrogen) was co-expressed with the 5-HT_{3A} receptor subunits to permit selection of transfected cells under fluorescence optics. Each 35 mm dish was transfected with 3 μg of cDNA encoding the wild-type or mutant receptors along with 1 μg of cDNA encoding green fluorescent protein.

Whole-cell patch-clamp recording

Whole-cell recordings were performed in HEK 293 cells 1–3 day after transfection. Cells were re-plated on the day of the experiment and continuously superfused with a solution containing 140 mM NaCl, 5 mM KCl, 1.8 mM $CaCl_2$, 1.2 mM $MgCl_2$, 5 mM glucose and 10 mM Hepes (pH was adjusted to 7.4 with NaOH and osmolarity adjusted to ~340 mosmol l^{-1} with sucrose). In some experiments, $CaCl_2$ in the external solution was either reduced or increased without NaCl compensation. The liquid junction potential was not corrected. Pipettes were pulled from borosilicate glass (TW-150F, World Precision Instruments, Sarasota, FL, USA) using a two-stage puller (Flaming-Brown P-97; Sutter Instruments, Novato, CA, USA) and had resistances of 2–5 MΩ when filled with pipette solution containing 140 mM CsCl, 2 mM $MgCl_2$, 10 mM EGTA, 10 mM Hepes (pH 7.2 adjusted with CsOH and osmolarity adjusted to ~315 mosmol l^{-1} with sucrose). In one experiment examining the D298R construct, CsCl in the pipette solution was replaced with equimolar Cs-$MeSO_3$ to assess if reversal potential was altered by reducing $[Cl^-]_i$. Membrane current was recorded in the whole-cell configuration (Hamill *et al.* 1981) using an Axopatch 200B amplifier (Axon Instruments, Foster City, CA, USA) at 20–22°C. Only cells with a capacitance of 8–12 pF, isolated from neighbouring cells, were used for experiments. Cells were held at −60 mV unless otherwise indicated.

Data were acquired using pCLAMP 9.0 software (Axon). Currents were filtered at 2 kHz and digitized at 5–10 kHz. Agonists were applied with a piezoelectric device (PZ-150M; EXFO Burleigh Products Group Inc., Victor, NY, USA) through two-barrelled theta glass tubing (TGC150, Warner Instruments, Hamden, CT, USA) that had been pulled to a tip diameter of ~200 μm. The cell was placed in front of the stream of control solution. The piezoelectric device was driven by TTL pulses from the pCLAMP 9.0 software. Voltage applied to the piezoelectric device produced a rapid lateral displacement (~50 μm) of the theta tubing to move the interface between control and agonist solutions. Solution exchange rate for open pipette and whole-cell recording was estimated using the potential change induced by switching from the control solution to a 140 mM *N*-methyl-D-glucamine (NMDG) test solution at 0 mV in the absence of agonist; the current rising phase was fitted using an exponential function. The solution exchange time constants were ~0.3 ms for an open pipette tip and ~1.6 ms for whole-cell recording.

Data analysis

Data analysis and curve fitting were performed with Origin 7.0 (Microcal Software, Northampton, MA, USA), pCLAMP 9.0 (Axon), or GraphPad InStat 3.0 (GraphPad Software Inc., San Diego, CA, USA) software. Concentration–response data were fitted using the Hill equation:

$$I/I_{max} = 1/\left[1 + (EC_{50}/[\text{Agonist}])^{nH}\right]$$

where I is the current amplitude activated by a given concentration of agonist ([Agonist]), I_{max} is the maximum response of the cell, nH is the Hill coefficient and EC_{50} is the concentration eliciting a half-maximal response.

Parameters of channel activation, deactivation and desensitization were estimated by fitting appropriate current components using exponential functions of the general form:

$$\Sigma A_n e^{(-t/\tau_n)} + A_s$$

where A_n is the relative amplitude of the respective component, A_s is the steady-state current, n is the optimal number of exponential components, t is time and τ_n is the respective time constant. Curve fitting was achieved in Clampfit 9.0 using the Levenberg-Marquardt algorithm. Additional components were accepted only if they significantly improved the fit, as determined by an F test performed by the analysis software.

Activation rates were derived from exponential fitting of the rising phase of agonist-activated current. Desensitization rates were derived from exponential fits to the current decay starting just after the current peak and extending to the end of agonist application. Deactivation rates were derived from exponential fits to the current decay after the removal of agonist following a 2 or 10 ms application of agonist. To facilitate direct comparison

of mono-exponentially and bi-exponentially fit data, a weighted summation of time constants ($\Sigma a_n \tau_n$) was used, where a_n is the fractional contribution of the respective component, τ_n is the respective time constant, and n is the optimal number of exponential components. The rate of current activation was also estimated by measuring the 10–30% slope of the initial inward current defined as the slope of a linear function fit to current between the time points at which current was 10 and 30% of the peak value (Zhou *et al.* 1998).

In some experiments voltage ramps were applied to measure reversal potential and provide an index of current rectification. A ramp with a slew rate of 0.5 mV ms^{-1} was applied during the peak of current activated by 3 μM 5-HT. Current activated by a voltage ramp in the absence of 5-HT was subtracted from the ramp-activated current in the presence of agonist prior to plotting and these data were analysed. Rectification index was determined using the equation:

$$\mathrm{RI} = \{[I_{+60}/(60 - E_{\mathrm{rev}})]/[I_{-60}/(-60 - E_{\mathrm{rev}})]\}$$

where I_{+60} and I_{-60} were the amplitude of 5-HT-activated currents at holding potentials of +60 mV and −60 mV, respectively, and E_{rev} is the reversal potential determined for the cell under study.

Data are presented as mean ± S.E.M. Statistical significance was determined with Student's t test or one-way analysis of variance (ANOVA). Differences were considered significant at $P < 0.05$.

Results

D298 mutation effects on apparent affinity for 5-HT and *I–V* relationship

Three mutant 5-HT$_{3A}$ receptors were constructed. D298 was either replaced with alanine to neutralize the charge, glutamate to maintain the negative charge, or arginine to reverse the charge. Transfection of all mutant receptor cDNAs into HEK 293 cells resulted in the functional expression of 5-HT$_{3A}$ receptors when examined using whole-cell patch-clamp recording. At a holding potential of −60 mV, application of a maximally efficacious concentration of the full agonist, 5-HT (30 μM), for 250 ms activated a rapidly rising inward current in the wild-type and mutant receptors (Fig. 1*C*). Upon removal of the agonist, the current decay appeared to be faster in the D298A and D298R receptors, but slower in the D298E receptor than in the wild-type receptor. It should be noted that the maximal current activated by 30 μM 5-HT in the wild-type, D298A and D298E receptors was comparable when transfected with equal amount of 5-HT$_{3A}$ receptor cDNA (wild-type: −1542 ± 101 pA, $n = 81$; D298A: −1802 ± 123 pA, $n = 72$; and D298E: −1507 ± 87 pA, $n = 58$; ANOVA, $P = 0.11$). However, maximal current amplitude was much smaller in the D298R receptor (−297 ± 31 pA, $n = 63$, $P < 0.001$).

To further characterize the effect of the D298 mutations on functional properties of the receptors, concentration–response relationships for 5-HT were constructed for the wild-type and mutant receptors (Fig. 1*D*). The concentration–response curve for 5-HT was shifted to the right by the D→A and D→R mutations, but was not altered by the D→E mutation. Fitting data with the Hill equation revealed that the EC_{50} values were 1.74 ± 0.09, 3.05 ± 0.14, 1.84 ± 0.10 and 7.20 ± 0.20 μM for the wild-type, D298A, D298E and D298R receptors, respectively. The Hill coefficients were 1.99 ± 0.11, 1.98 ± 0.09 and 1.99 ± 0.04 for the D298A, D298E, and D298R receptors, respectively, which are not different from that for the wild-type receptor (1.99 ± 0.05, ANOVA, $P = 0.8$). These results suggest that agonist stoichiometry/cooperativity was not changed by the D298 mutations.

Figure 1*E* depicts current–voltage (*I–V*) relationships obtained by applying a voltage ramp from −80 to +60 mV at the peak of current activated by 3 μM 5-HT in the wild-type and mutant receptors. 5-HT activated inward current at negative membrane potentials, and the current became outward at positive membrane potentials. The shape of the *I–V* relationship was similar for the wild-type and mutant receptors. The current reversed at 4.2 ± 0.3, 4.8 ± 0.6 and 4.6 ± 0.4 mV for the D298A, D298E and D298R receptors, respectively, and those values are almost identical to that for the wild-type receptor (4.8 ± 0.4 mV; ANOVA, $P = 0.7$). The rectification indices were 0.77 ± 0.03, 0.71 ± 0.07, 0.75 ± 0.02 and 0.31 ± 0.02 for the wild-type, D298A, D298E and D298R receptors, respectively, suggesting that inward rectification of the 5-HT$_{3A}$ receptor-mediated current was not altered in most of the mutant receptors, but was slightly enhanced by the D298R mutation. When chloride in the internal solution was replaced with methanesulphonate, similar reversal potential (5.3 ± 0.4 mV, $P = 0.2$) and rectification index (0.30 ± 0.04, $P = 0.5$) values were obtained for the D298R receptor.

D298 mutations do not alter antagonist effects

Mutations of ligand-gated ion channels might result in spontaneous receptor activation in the absence of agonist. Spontaneous opening can be detected by applying antagonists in the absence of agonist (Chang & Weiss, 1998; Bianchi & Macdonald, 2001; Scheller & Forman, 2002). In cells expressing the wild-type receptor application of 300 nM MDL 72222, a competitive 5-HT$_3$ receptor antagonist, for 10 s in the absence of 5-HT did not alter the holding current (data not shown). Similarly, in cells expressing either the

D298A or D298E receptor the application of 300 nM MDL 72222 for 10 s also failed to alter the holding current. We also tested the effectiveness of MDL 72222 in antagonizing 5-HT-activated currents. MDL 72222 at 300 nM completely blocked the currents activated by 30 μM 5-HT in the wild-type and mutant receptors. Furthermore, we found that there was no significant difference in the resting current level at −60 mV observed in cells expressing the wild-type and mutant receptors in the absence of 5-HT (wild-type: -18.1 ± 1.1 pA; D298A: -19.5 ± 1.1 pA; D298E: -18.6 ± 1.3 pA and D298R: -19.9 ± 1.2 pA; ANOVA, $P = 0.7$). Taken together, our data confirm that the 5-HT-activated currents are due to activation of the 5-HT_{3A} receptor, and suggest that D298 mutations do not induce spontaneous opening of the channel.

D298 mutations alter 5-HT_{3A} receptor activation

The time course of 5-HT_{3A} receptor activation was investigated over a range of concentrations of 5-HT (0.3 μM−1 mM). Typical responses activated by 3 μM (upper) and 30 μM (lower) 5-HT are shown in Fig. 2*A*, and the current amplitudes have been normalized for comparison. Plotting the reciprocal of the activation time constant ($1/\tau_{act}$) as a function of 5-HT concentration illustrates significant concentration-dependent differences in activation rate in the wild-type and mutant receptors (Fig. 2*B*). The activation rate of the D298A receptor was faster than that of the wild-type receptor at all concentrations examined, whereas the activation rate for the D298E receptor was similar to that of the wild-type receptor at 5-HT concentrations ≤ 30 μM. The maximal activation rate in response to a saturating concentration of 5-HT (1 mM, Hu *et al.* 2003) was altered by the D298 mutations (ANOVA, $P < 0.01$). The D→A mutation created a receptor with a maximal activation rate faster than that in the wild-type receptor. In contrast, the D→E mutation resulted in a receptor exhibiting a maximal activation rate slower than that observed in the wild-type receptor. Only the activation in response to 1 mM 5-HT was measured in the D298R receptor; and the kinetics at lower concentrations of the agonist were not determined due to insufficient current amplitude. The activation time constant for the D298R receptor was 4.0 ± 0.2 ms for 1 mM 5-HT, which is significantly different from that of the wild-type receptor which was 7.1 ± 0.4 ms (Student's *t* test, $P < 0.01$). In addition, the concentration of 5-HT producing half-maximal activation rate was altered by the D298 mutations. The 5-HT concentration needed to achieve half-maximal activation rate was similar in the wild-type and D298E receptors (wild-type: 27.9 ± 1.3 μM; D298E: 22.4 ± 0.7 μM); whereas only 12.1 ± 1.2 μM 5-HT was required to achieve half-maximal activation rate in the D298A receptor (ANOVA, $P < 0.01$). Current amplitudes for the D298R receptor were too small to permit accurate measurement of activation over a wide range of agonist concentrations, and thus we did not include activation rate data for this mutant receptor.

To obtain an alternative measure of current activation uncontaminated by desensitization the slope of the initial rising phase of current between 10 and 30% of the peak current amplitude was also determined for the wild-type and mutant receptors as previously described (Zhou *et al.* 1998). The 10–30% slope of current activated by 3 μM 5-HT (wild-type: -5.9 ± 2 pA ms^{-1}; D298A: -12.5 ± 2 pA ms^{-1}; D298E: -3.7 ± 1.3 pA ms^{-1}, ANOVA, $P < 0.002$) and 30 μM 5-HT (wild-type: -92.3 ± 14.7 pA ms^{-1}; D298A: -184.1 ± 25.2 pA ms^{-1}; D298E: -72.2 ± 15.1 pA ms^{-1}, ANOVA, $P < 0.001$) differed among the different constructs. Whereas the slopes were similar in the wild-type and D298E receptors ($P > 0.05$), the D298A receptor exhibited a 2- to 3-fold increase in the slope relative to the wild-type and D298E receptors ($P < 0.01$).

D298 mutations alter desensitization and deactivation of 5-HT-activated current

Desensitization and deactivation are two processes that terminate ion flow through ligand-gated ion channels. Desensitization is the process of channel closing in an agonist-bound state, measured in the continuous presence

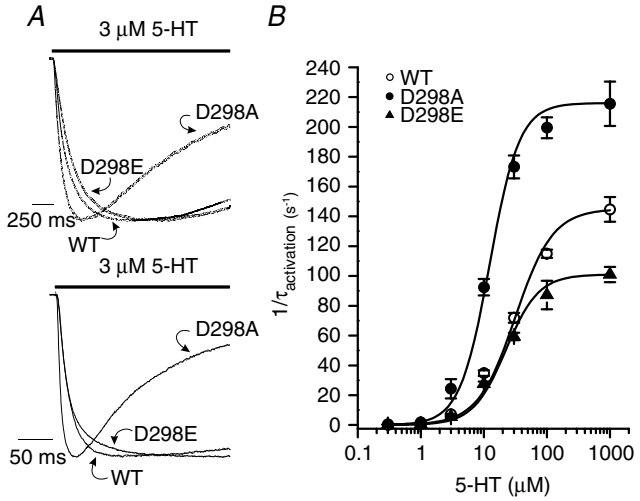

Figure 2. D298 mutations alter 5-HT_{3A} receptor activation kinetics
A, traces show receptor activation elicited by 3 μM (upper) and 30 μM (lower) 5-HT. The responses were normalized to peak current for comparison. The bar indicates the time of agonist application. *B*, plot of the activation rate ($1/\tau_{act}$) *versus* 5-HT concentration. Each data point represents mean ± S.E.M. from 8 to 55 cells.

of agonist. Deactivation represents agonist unbinding and channel closing after removal of agonist. We examined desensitization kinetics during a long pulse (10 s) of 30 μM 5-HT and deactivation kinetics following a brief pulse (2 ms) of 1 mM 5-HT in cells transfected with the wild-type and mutant receptors (Fig. 3). Current decay during and after agonist application was well described by an exponential process in the WT and all mutant constructs. No evidence of current rebound was observed following removal of agonist.

Examples of desensitization resulting from the application of 30 μM 5-HT are shown in Fig. 3*A*. The current mediated by all receptors activated rapidly in response to 5-HT and then decayed exponentially in the continuous presence of the agonist. Desensitization time course was best fitted by a mono-exponential function in the wild-type, D298E and D298R receptors, but decay was bi-exponential for the D298A receptor (Table 1). The fast phase of desensitization introduced by the D298A mutation accounted for ~70% of the current amplitude. To facilitate comparison of desensitization among receptors, we compared the weighted desensitization kinetics. Analysis of weighted desensitization time constant values ($\tau_{\text{wted desens}}$) revealed that the D→A and D→R mutations produced a significant alteration in desensitization rate of the 5-HT$_{3A}$ receptors (ANOVA, $P < 0.001$). Although the rates of desensitization in the wild-type and D298E receptors were comparable ($P > 0.05$), the rate of desensitization in the D298A and D298R receptors was considerably faster than in the wild-type ($P < 0.001$) and D298E ($P < 0.001$) receptors. In the continuous presence of 5-HT, the desensitization caused approximately 80% current loss in the wild-type and D298E receptors at the end of the agonist application. However, the current decayed nearly completely back to pre-agonist baseline levels in the D298A and D298R receptors (Fig. 3*A*). Our results demonstrate that desensitization is accelerated by the D→A and D→R mutations, whereas the D→E mutation creates a receptor with properties closely resembling those of the wild-type receptor.

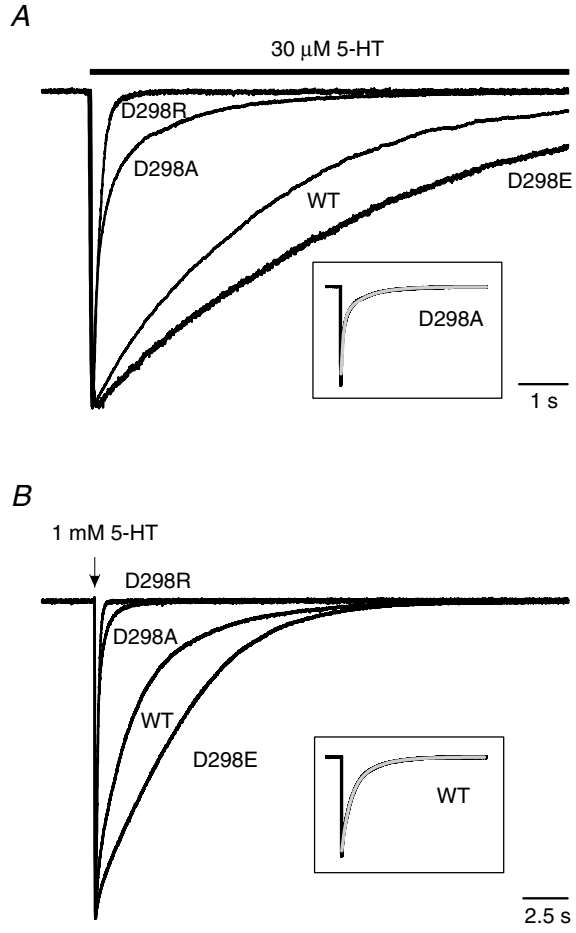

Figure 3. D298 mutations alter desensitization and deactivation of 5-HT-activated current
A, traces show desensitization of 30 μM 5-HT-activated current. The bar indicates the time of agonist application. *B*, traces show deactivation after termination of 2 ms application of 1 mM 5-HT. The arrow indicates the brief application of 5-HT. Currents were normalized to peak current and superimposed for comparison of desensitization and deactivation. Time constants for desensitization and deactivation were estimated by fitting with either a mono-exponential (WT, D298E and D298R) or a bi-exponential (D298A) function. Examples of exponential fits are presented in the boxed insets in grey. Data are summarized in Table 1.

After rapid application and removal of agonist, the current activated by 1 mM 5-HT decayed exponentially back to baseline in the wild-type and mutant receptors (Fig. 3*B*). The overlaid traces in Fig. 3*B*, normalized with respect to peak current amplitude, reveal that current decayed much faster in the D298A and D298R receptors than in the wild-type and D298E receptors. Current deactivation was well fitted with a mono-exponential function for the wild-type, D298E and D298R receptors, but a bi-exponential function was required for adequate fitting of deactivation of the D298A receptor (Table 1). The fast phase of deactivation in the D298A receptor represented ~70% of the current decay. The weighted deactivation time constant ($\tau_{\text{wted deact}}$) was significantly altered by the D298 mutations (Table 1, ANOVA, $P < 0.01$). The D→A or D→R mutations produced receptors that exhibited a dramatically faster deactivation rate than that observed in the wild-type receptor ($P < 0.01$), whereas the D→E mutant receptor exhibited a marginally slower deactivation rate than in the wild-type receptor ($P < 0.06$).

D298 mutation effects on properties of partial agonists

Both 2-Me-5-HT and dopamine are partial agonists at the mouse 5-HT$_3$ receptor (van Hooft & Vijverberg,

Table 1. Desensitization and deactivation kinetics of 5-HT-activated currents

	τ_{fast} (ms)	% Fast	τ_{slow} (ms)	% Slow	$\tau_{weighted}$ (ms)	*n*
Desensitization						
WT	—	—	3365 ± 162	100	3365 ± 162	20
D298A	205 ± 17	72 ± 3	1499 ± 63	28 ± 3	565 ± 41**	24
D298E	—	—	4258 ± 537	100	4258 ± 537	22
D298R	200 ± 15	100	—	—	200 ± 15**	15
Deactivation						
WT	—	—	3232 ± 218	100	3232 ± 218	19
D298A	147 ± 7.4	74 ± 2	926 ± 57	26 ± 2	337 ± 20**	31
D298E	—	—	4032 ± 324	100	4032 ± 324	23
D298R	122 ± 8	100	—	—	122 ± 8**	13

All data are given as mean ± S.E.M. $^{**}P < 0.01$, compared to WT.

1996; Hu *et al.* 2003). Since the efficacy of an agonist is essentially determined by the isomerization process between the agonist-bound closed and open states (Colquhoun, 1998), a change in gating would probably alter efficacy of a partial agonist. We compared the responses evoked by a maximally efficacious concentration of either 2-Me-5-HT (100 μM) or dopamine (3 mM) with the current amplitude activated by 30 μM 5-HT in the wild-type and mutant receptors (Fig. 4). The D→A mutation dramatically reduced the relative amplitude of currents activated by 2-Me-5-HT (Fig. 4*A*) and dopamine (Fig. 4*B*). In contrast, the responses to the partial agonists with the conservative D→E replacement were comparable to the wild-type receptor. Averaged data revealed that the D→A mutation reduced the efficacies of 2-Me-5-HT and dopamine relative to 5-HT, whereas the D→E

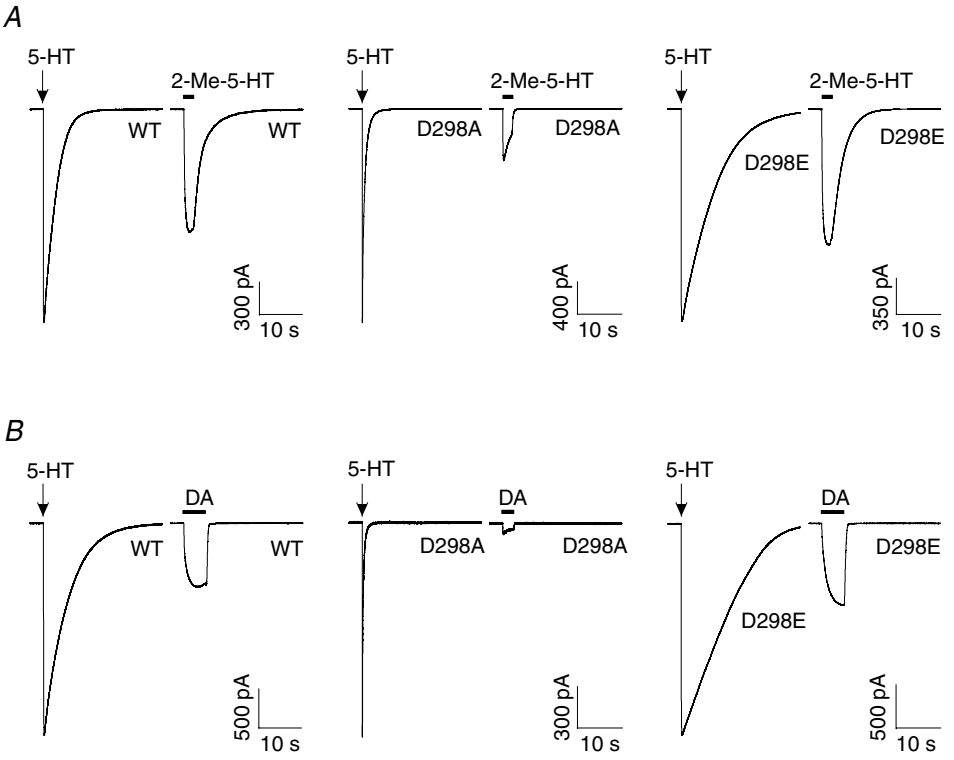

Figure 4. D298 mutations alter the relative efficacy of partial agonists
Traces show currents activated by partial agonists, 2-Me-5-HT (*A*) and dopamine (DA, *B*). The cells expressing the WT and mutant receptors were first exposed to 30 μM 5-HT. After complete washout of the agonist, the cells were challenged with either 100 μM 2-Me-5-HT or 3 mM DA. The relative efficacy of the partial agonists was determined by normalizing the current amplitude activated by partial agonists as a percentage of that activated by 30 μM 5-HT.

mutation increased the relative efficacy of 2-Me-5-HT (wild-type: 54.7 ± 2.9%; D298A: 21.1 ± 2.4%; and D298E: 66.8 ± 2.2%, ANOVA, $P < 0.01$; D298A *versus* wild-type, $P < 0.01$; D298E *versus* wild-type, $P < 0.01$) and produced no significant change in the relative efficacy of dopamine (wild-type: 29.9 ± 1.7%, D298A: 7.7 ± 1.2%; and D298E: 35.5 ± 3.8%, ANOVA, $P < 0.01$; D298A *versus* wild-type, $P < 0.01$; D298E *versus* wild-type, $P > 0.05$). When tested at a holding potential of +40 mV, the relative efficacy for dopamine was 30.3 ± 3.9% for the wild-type receptor ($n = 7$) and 5.3 ± 0.9% for the D298A receptor ($n = 8$), which are not different from the aforementioned values obtained at a holding potential of −60 mV (wild-type, $P = 0.9$; D298A, $P = 0.2$). Given that the maximal response of D298R to 5-HT was small, it was not possible to accurately assess responses to partial agonists in this mutant receptor.

We subsequently examined the kinetics of partial agonist-activated current in the wild-type and mutant receptors. In response to either 2-Me-5-HT (100 μM) or dopamine (3 mM), activation of the D298A receptor was much faster than that of the wild-type and D298E receptors (Fig. 5*A*). 2-Me-5-HT or dopamine activated a relatively slowly desensitizing current in the wild-type and D298E receptors and a faster desensitizing current in the D298A receptor (Fig. 5*B*). The deactivation of currents activated by either 2-Me-5-HT or dopamine was well fitted by a mono-exponential function in the wild-type and mutant receptors. However, deactivation in the D298A receptor appeared to be faster than the wild-type and D298E receptors (Fig. 5*C*). Overall, the D298 mutations produced significant changes in the rates of activation, desensitization and deactivation for both partial agonists (Table 2; D298A > wild-type > D298E, ANOVA, $P < 0.001$).

D298 mutations alter modulation of 5-HT$_{3A}$ receptors by extracellular Ca^{2+}

Current mediated by 5-HT$_3$ receptors is sensitive to changes in extracellular calcium (Peters *et al.* 1988). Negatively charged amino acid residues such as aspartate and glutamate have been found to play a role in cation modulation of G protein-coupled receptors (Ceresa & Limbird, 1994) and ion channels (Johnson *et al.* 2001; Watanabe *et al.* 2002). Thus, we hypothesized that D298 may participate in modulation of the 5-HT$_{3A}$ receptor by extracellular Ca^{2+}, and examined the modulatory effect of changing extracellular Ca^{2+} on the wild-type and mutant receptors.

Effects of increasing $[Ca^{2+}]_o$ from 1.8 to 10 mM on 3 μM and 30 μM 5-HT-activated currents were examined. Current activated by both concentrations of 5-HT was reduced by the increase in $[Ca^{2+}]_o$ in the wild-type and D298E receptors, whereas it appeared to be unaltered in the D298A and D298R receptors (Fig. 6*A*). Pooled data indicated that Ca^{2+} inhibition in the wild-type and D298E receptors was more prominent at the lower agonist

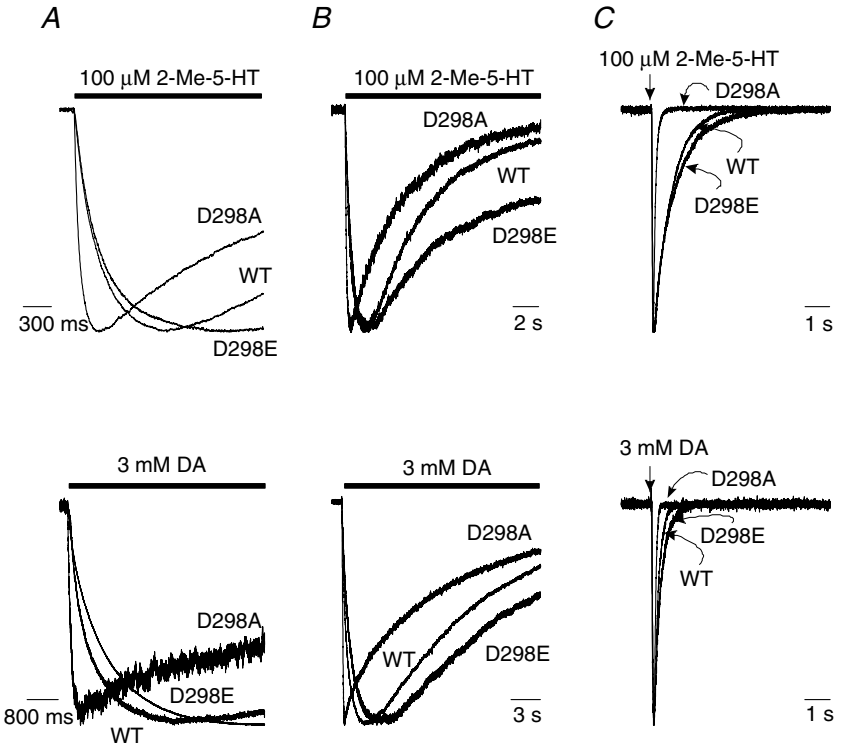

Figure 5. Alterations of kinetics of partial agonist-activated currents by the D298 mutations
Traces show kinetics of currents activated by partial agonists, 2-Me-5-HT (100 μM) and dopamine (3 mM). *A*, activation elicited by 2-Me-5-HT (upper) and DA (lower). *B*, desensitization of currents activated by 2-Me-5-HT for 15 s (upper) and 3 mM DA for 20 s (lower). *C*, deactivation of currents activated by 2-Me-5-HT (upper) and DA for 10 ms (lower). The bar indicates the time of agonist application for activation and desensitization studies, and the straight arrow indicates the time point of application of agonists for 10 ms for deactivation study. Data are summarized in Table 2.

Table 2. Kinetics of partial agonist-activated currents

	Activation		Desensitization		Deactivation	
	τ (ms)	n	τ (ms)	n	τ (ms)	n
2-Me-5-HT						
WT	259 ± 14	13	5653 ± 383	10	633 ± 38	14
D298A	$54 \pm 6^{**}$	11	$3462 \pm 223^{**}$	14	$101 \pm 5^{**}$	11
D298E	$298 \pm 12^{*}$	15	$9730 \pm 1352^{**}$	8	$879 \pm 53^{**}$	11
Dopamine						
WT	543 ± 18	10	17967 ± 2575	9	184 ± 15	10
D298A	$48 \pm 6^{**}$	21	$5685 \pm 761^{**}$	11	$69 \pm 4^{**}$	7
D298E	$832 \pm 70^{**}$	14	23794 ± 2644	10	$273 \pm 17^{**}$	9

All data are given as mean ± S.E.M. $^{*}P < 0.05$, $^{**}P < 0.01$, compared to WT.

concentration than at the higher concentration: ∼65% at 3 μM and ∼25% at 30 μM 5-HT, and this inhibition was not observed in the D298A and D298R receptors (Fig. 6*B*). Figure 6*C* depicts *I–V* relationships obtained at the peak current evoked by 3 μM 5-HT in 1.8 and 10 mM $[Ca^{2+}]_o$. Increasing $[Ca^{2+}]_o$ caused a voltage-independent reduction of current amplitude in both the wild-type and D298E receptors, whereas it resulted in no change in the D298A and D298R receptors. The reversal potentials of 5-HT-activated currents in the wild-type and mutant receptors were not altered by increasing $[Ca^{2+}]_o$ (Fig. 6*D*, ANOVA, $P = 0.5$). The rectification indices were 0.74 ± 0.06, 0.70 ± 0.06, 0.72 ± 0.05 and 0.33 ± 0.04 for the wild-type, D298A, D298E and D298R receptors, respectively, in 10 mM $[Ca^{2+}]_o$.

Increasing $[Ca^{2+}]_o$ from 1.8 mM to 10 mM accelerated receptor activation in response to a saturating 5-HT concentration (1 mM) in both the wild-type and D298E receptors, whereas activation rate appeared to be unaltered in the D298A receptor (Fig. 7*A*, upper). As shown in Fig. 7*B* (upper panel), averaged data revealed that activation rate was significantly faster in 10 mM $[Ca^{2+}]_o$ than in 1.8 mM $[Ca^{2+}]_o$ for both the wild-type and D298E receptors ($P < 0.001$), whereas activation rate was similar for the D298A receptor in 1.8 and 10 mM $[Ca^{2+}]_o$ ($P = 0.8$). In addition, activation of the receptor in response to 30 μM 5-HT was also accelerated by increasing $[Ca^{2+}]_o$ from 1.8 to 10 mM (wild-type: 17.9 ± 1.3 to 8.1 ± 0.7 ms, $n = 15$, $P < 0.001$; D298E: 22.3 ± 3.1 to 10.6 ± 1.5 ms, $n = 8$, $P < 0.002$). In contrast, such an acceleration in activation was not observed in the D298A receptor (8.3 ± 0.3 to 8.5 ± 0.3 ms, $n = 5$, $P = 0.6$) when $[Ca^{2+}]_o$ was increased from 1.8 to 10 mM.

As described above, the desensitization of 30 μM 5-HT-activated current in 1.8 mM $[Ca^{2+}]_o$ followed a mono-exponential time course for the wild-type, D298E and D298R receptors, but a bi-exponential function for the D298A receptor (Fig. 7*A*, middle panel). When $[Ca^{2+}]_o$ was elevated from 1.8 to 10 mM, desensitization was accelerated for the wild-type and D298E receptors, and was now better described by a bi-exponential function. In contrast, desensitization of the D298A or D298R receptor was not apparently altered with such an increase in $[Ca^{2+}]_o$. Averaged data revealed that the rate of desensitization in 10 mM $[Ca^{2+}]_o$ for the wild-type and D298E receptors was significantly increased relative to that in 1.8 mM $[Ca^{2+}]_o$ (Fig. 7*B*, middle, $P < 0.01$), whereas the rate of desensitization in 10 mM $[Ca^{2+}]_o$ was not different from that observed in 1.8 mM $[Ca^{2+}]_o$ for the D298A ($P = 0.7$) and D298R ($P = 0.2$) receptors.

The deactivation of current after a brief exposure (2 ms) to 1 mM 5-HT was mono-exponential in the wild-type, D298E and D298R receptors, and bi-exponential in the D298A receptor in 1.8 mM $[Ca^{2+}]_o$, as previously mentioned. Deactivation appeared to be bi-exponential and increased in rate when $[Ca^{2+}]_o$ was increased from 1.8 to 10 mM in the wild-type and D298E receptors, whereas deactivation rate appeared to be similar in the presence of 1.8 and 10 mM $[Ca^{2+}]_o$ for the D298A and D298R receptors (Fig. 7*A*, lower panel). Pooled data demonstrated that deactivation rate was markedly accelerated in both the wild-type and D298E receptors by increasing $[Ca^{2+}]_o$ from 1.8 to 10 mM (Fig. 7*B*, lower, $P < 0.001$), whereas it remained unchanged in the D298A ($P = 0.8$) and D298R ($P = 0.2$) receptors.

We also examined the effect of lowering $[Ca^{2+}]_o$ from 1.8 to 0.1 mM on 5-HT_{3A} receptor-mediated currents. As shown in Fig. 8*A* and *B*, lowering $[Ca^{2+}]_o$ enhanced 3 μM 5-HT-activated currents by ∼25% in both the wild-type and D298E receptors, whereas this enhancement was not present in the D298A receptor. The desensitization and deactivation of 5-HT-activated currents were slowed when $[Ca^{2+}]_o$ was lowered from 1.8 to 0.1 mM in the wild-type and D298E receptors ($P < 0.01$). In contrast, both kinetic measures were similar in 1.8 and 0.1 mM $[Ca^{2+}]_o$ for the D298A receptor (Fig. 8*C* and *D*; $P = 0.3$).

Discussion

Several studies have provided strong evidence that the TM2–TM3 loop contributes to the coupling process between agonist binding and channel gating

in ligand-gated ion channels (Rajendra *et al.* 1995; Campos-Caro *et al.* 1996; Lynch *et al.* 1997; Rovira *et al.* 1998, 1999; O'Shea & Harrison, 2000; Absalom *et al.* 2003; Kash *et al.* 2003). Our findings concerning aspartate 298 of the 5-HT_{3A} receptor support this idea, and indicate that the negative charge at this residue participates in determining the kinetics of channel gating. In addition, this negative charge appears to be a crucial determinant of voltage-independent $[Ca^{2+}]_o$ modulation of the 5-HT_{3A} receptor.

Activation of ligand-gated ion channels consists of at least two steps: binding of the agonist to the receptor and conformational changes that move the protein from the bound closed state to the bound open state (Colquhoun, 1998). An alteration in activation rate suggests a change in either agonist affinity or gating, or both. It has been shown that activation kinetics are determined by the rate constant of the transition from the closed to open states (β) at a saturating concentration of agonist (Maconochie & Steinbach, 1998). We have previously demonstrated that the activation rate of the wild-type 5-HT_{3A} receptor reaches its maximum at 300 μM 5-HT (Hu *et al.* 2003). In this study, the activation rate in response to a saturating concentration of 5-HT (1 mM) was found to be enhanced

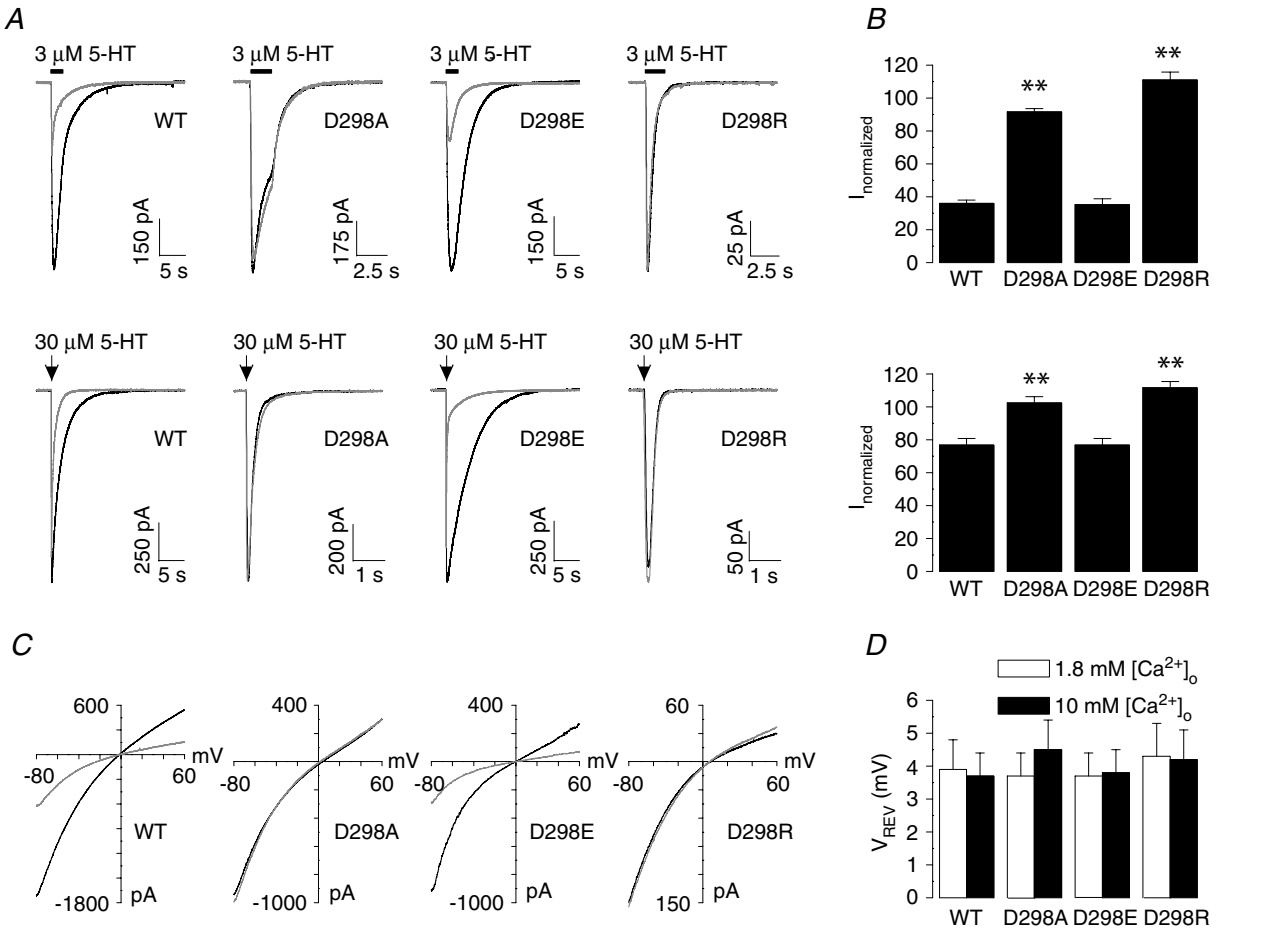

Figure 6. Modulation of 5-HT-activated currents and *I–V* relationships by increasing $[Ca^{2+}]_o$ in the WT and mutant receptors

A, traces show currents activated by 3 μM (upper) and 30 μM 5-HT (lower) in 1.8 and 10 mM $[Ca^{2+}]_o$. Cells expressing the WT and mutant receptors were first exposed to 5-HT in 1.8 mM $[Ca^{2+}]_o$ followed by complete washout of the agonist. Cells were then incubated in 10 mM $[Ca^{2+}]_o$ and exposed to the same concentration of agonist again. Note that the traces for the D298A and D298R receptors have faster time scale and the traces in 1.8 and 10 mM $[Ca^{2+}]_o$ are almost completely superimposed. *B*, averaged data show effects of increasing $[Ca^{2+}]_o$ on currents activated by 3 μM (upper) and 30 μM (lower) 5-HT. The current amplitude in 10 mM $[Ca^{2+}]_o$ was normalized to that in 1.8 mM $[Ca^{2+}]_o$. Each bar represents mean ± S.E.M. from 5 to 20 cells. *C*, voltage ramp obtained at the peak of current activated by 3 μM 5-HT first in 1.8 mM $[Ca^{2+}]_o$ then in 10 mM $[Ca^{2+}]_o$. Currents activated by the voltage protocol in the absence of 5-HT have been subtracted. *D*, averaged data show the reversal potentials (E_{rev}) of 5-HT-activated currents. Each bar represents mean ± S.E.M. from 5 to 7 cells. ** $P < 0.01$. The traces obtained in 1.8 mM $[Ca^{2+}]_o$ are in black, whereas those obtained in 10 mM $[Ca^{2+}]_o$ are in grey.

by the D→A mutation, but depressed by the D→E mutation. The accelerated channel opening suggests an increase in gating kinetics due to the D→A mutation. This finding suggests that the D298 residue participates in determining the stability of the closed and open conformations of the 5-HT_{3A} receptor. This is consistent with data from past studies in which mutations in the TM2–TM3 loop have been associated with an alteration in gating rather than binding in the glycine receptor (Lewis *et al.* 1998) and nACh receptors (Campos-Caro *et al.* 1996; Rovira *et al.* 1998, 1999; Grosman *et al.* 2000).

The D298A and D298R receptors displayed a marked increase in the rate of desensitization. In contrast, the wild-type and D298E receptors exhibit comparable desensitization rates. These data suggest that the open state is more unstable in the D298A and D298R receptors than in the wild-type and D298E receptors. Thus, D298 mutations also alter the relative stability of the open and desensitized states. The relationship between agonist-binding/activation and desensitization has been well established in the nACh receptors (Auerbach & Akk, 1998) and $GABA_A$ receptors (Jones & Westbrook, 1995; Scheller & Forman, 2002). The concomitant changes in activation and desensitization resulting from the D298 mutations point to a positive coupling between these two events in the 5-HT_{3A} receptor, which is consistent with

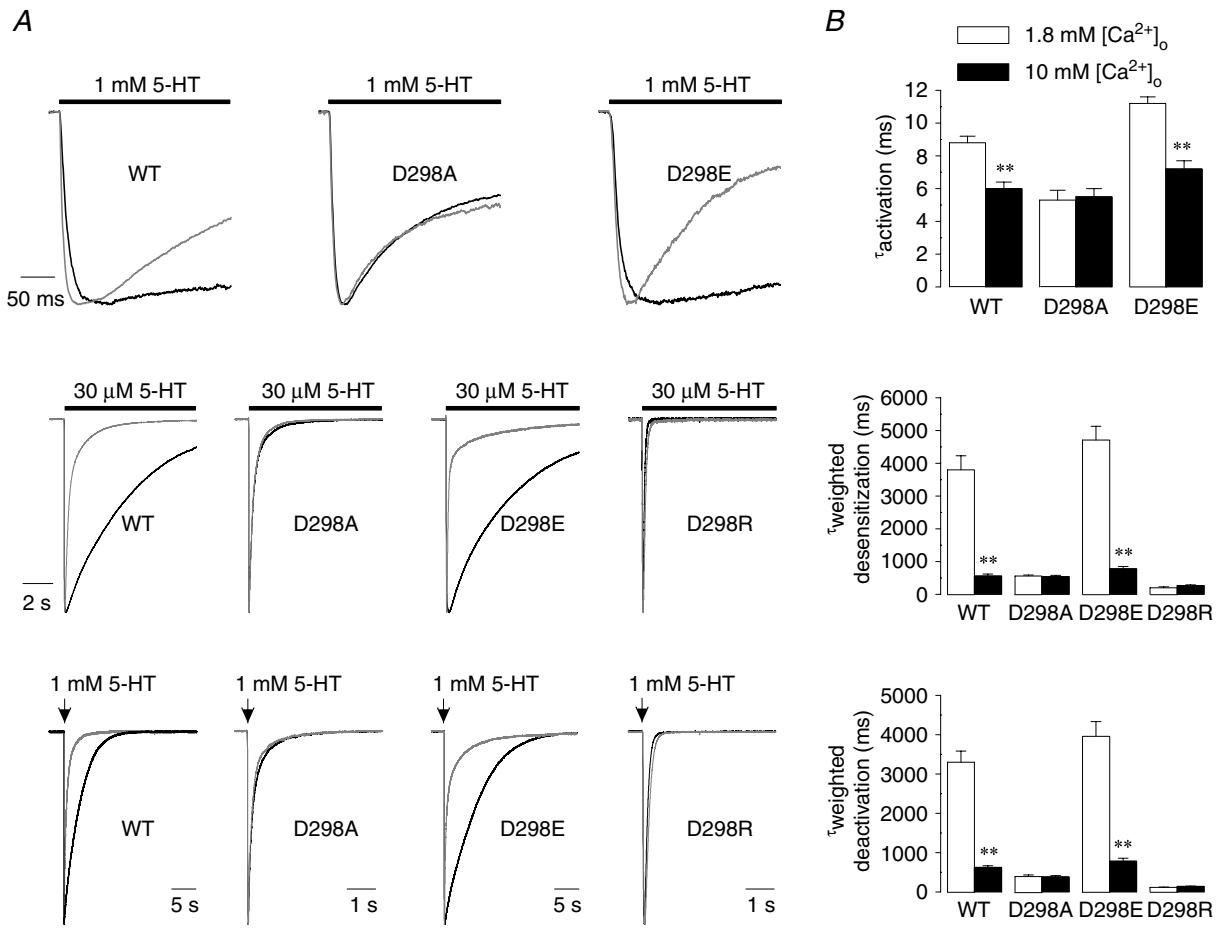

Figure 7. Effects of increasing $[Ca^{2+}]_o$ on the kinetics of 5-HT-activated currents in the WT and mutant receptors

A, traces show alteration in activation, desensitization and deactivation by increasing $[Ca^{2+}]_o$ from 1.8 to 10 mM (upper, receptor activation elicited by 1 mM 5-HT; middle, desensitization of 30 μM 5-HT-activated current; lower, deactivation after termination of 2 ms application of 1 mM 5-HT). Currents were normalized to peak current and superimposed for comparison. The bar indicates the time of agonist application, and the arrow indicates the time point of application of agonist for 2 ms. Note the overlapping of the desensitization traces for the D298A and D298R receptors in 1.8 and 10 mM $[Ca^{2+}]_o$. Also note that the deactivation traces for the D298A and D298R receptors have faster time scale and the traces in 1.8 and 10 mM $[Ca^{2+}]_o$ are almost completely superimposed. *B*, averaged data show the alteration in activation (upper), desensitization (middle) and deactivation (lower). Each bar represents mean ± S.E.M. from 7 to 14 cells. $^{**}P < 0.01$. The traces obtained in 1.8 mM $[Ca^{2+}]_o$ are in black, whereas those obtained in 10 mM $[Ca^{2+}]_o$ are in grey.

findings in studies of the nACh receptors (Auerbach & Akk, 1998) and confirms the results from our previous studies (Zhou *et al.* 1998; Hu *et al.* 2003). The alteration of desensitization by the D298 mutations further supports a role of this amino acid residue in the gating process of the 5-HT_{3A} receptor.

Accelerated deactivation could be caused by more rapid unbinding of agonist, which then would reduce the fraction of time spent in the open state and result in a rightward shift of the concentration–response curve. On the other hand, accelerated desensitization would increase the entry of the activated receptor into the desensitized state which would predict a leftward concentration–response shift. It is well known that the desensitized receptor state has higher affinity for agonist (Colquhoun, 1998), and thus the potency of agonist might be expected to increase if channels more rapidly enter the desensitized state. However, it should be noted that we determined agonist concentration–response functions using the peak current measure. It is most likely that only a small proportion of channels have entered the desensitized state at this time point. Thus, desensitization rate may have little influence on agonist potency determined using the peak current measure. We were unable to

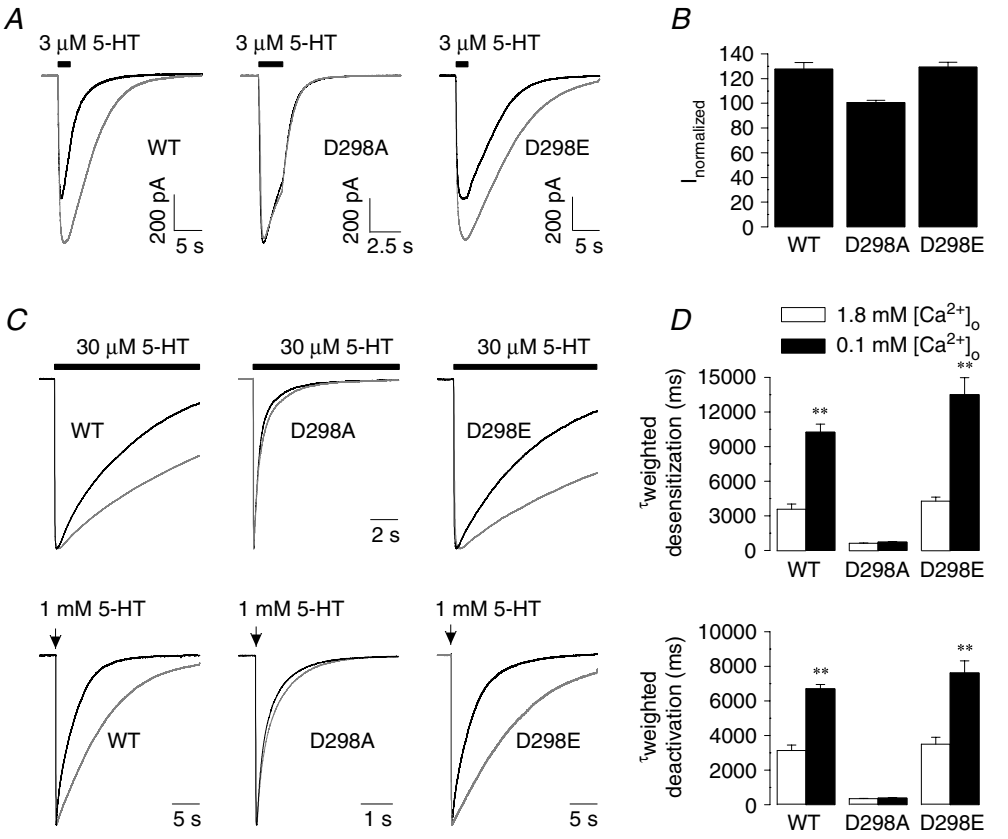

Figure 8. Effects of lowering $[Ca^{2+}]_o$ on the amplitude and kinetics of 5-HT-activated currents in the WT and mutant receptors

A, traces show currents activated by 3 μM 5-HT in 1.8 and 0.1 mM $[Ca^{2+}]_o$. The cells expressing the WT and mutant receptors were first exposed to 5-HT in 1.8 mM $[Ca^{2+}]_o$ followed by complete washout of the agonist. The cells were then incubated in 0.1 mM $[Ca^{2+}]_o$ and exposed to the same concentration of agonist again. Note that the traces for the D298A receptor have faster time scale and the traces in 1.8 and 0.1 mM $[Ca^{2+}]_o$ are almost completely superimposed. *B*, averaged data show effects of lowering $[Ca^{2+}]_o$ on current activated by 3 μM 5-HT-activated currents. The current amplitude in 0.1 mM $[Ca^{2+}]_o$ was normalized to that in 1.8 mM $[Ca^{2+}]_o$. Each bar represents mean ± S.E.M. from 9 to 17 cells. *C*, traces show alteration in desensitization and deactivation by lowering $[Ca^{2+}]_o$ from 1.8 to 0.1 mM (upper, desensitization of 30 μM 5-HT-activated current; lower, deactivation after termination of 2 ms application of 1 mM 5-HT). Currents were normalized to peak current and superimposed for comparison. The bar indicates the time of agonist application, and the arrow indicates the time point of application of agonist for 2 ms. Note that the deactivation traces for the D298A receptor have faster time scale and the traces in 1.8 and 0.1 mM $[Ca^{2+}]_o$ are almost completely superimposed. *D*, averaged data show the alteration in desensitization (upper) and deactivation (lower). Each bar represents mean ± S.E.M. from 6 to 8 cells. $^{**}P < 0.01$. The traces obtained in 1.8 mM $[Ca^{2+}]_o$ are in black, whereas those obtained in 0.1 mM $[Ca^{2+}]_o$ are in grey.

measure concentration–response curves for steady-state 5-HT-activated current because channel desensitization is nearly complete with prolonged application of agonist. Both deactivation and desensitization were accelerated in the D298A and D298R receptors. The net decrease in agonist potency that we observed in the D298A and D298R receptors is probably due to the fact that the increase in deactivation rate predominates relative to the increased desensitization rate in determining the concentration dependence of peak current.

Since the activation process is enhanced by the D→A mutation, we might also expect an increase in efficacy of the partial agonists 2-Me-5-HT and dopamine. However, we found that the efficacy of these partial agonists was decreased by the D→A mutation. The observation that the D→A mutation enhanced activation rate and reduced the efficacy of partial agonists might seem paradoxical. However, the maximal response is mainly determined by the net balance of two processes: the transition rate from the resting state to the open state; and the transition rate from the open state to the desensitized state. The desensitization of partial agonist-activated currents was much faster in the D298A receptor than in the wild-type receptor. Therefore, the quick entry into the desensitized state probably limits the efficacy of partial agonists despite facilitated activation in the D298A receptor.

Mutations at the residue corresponding to the D298 position in the *Torpedo* nACh receptor (Imoto *et al.* 1988) and glycine receptors (Langosch *et al.* 1994; Rajendra *et al.* 1995) resulted in decreased channel conductance. The markedly reduced amplitude of whole-cell current for the D298R receptor could be due to a reduction in channel conductance or a low abundance of receptor protein reaching the cell surface. The D→C mutation at this residue was previously found to produce a non-functional receptor without affecting cell surface expression (Reeves *et al.* 2001). We cannot rule out a similar possibility in the case of D298R, namely that some channels may be on the cell surface but non-functional or may exhibit very low probability of opening. The binding of Ca^{2+} to the D298 residue could also decrease the conductance of the channel. Such a mechanism has been proposed previously for Ca^{2+}-mediated inhibition of human 5-HT_{3A} receptor-mediated currents (Brown *et al.* 1998*b*). The negatively charged glutamate at the equivalent position of the *Torpedo* nACh receptor α subunit was found to be the site of Mg^{2+}-mediated reduction in channel conductance (Imoto *et al.* 1988). However, there are also mutations in the TM2–TM3 loop that are found to alter gating without changing the channel conductance in the glycine (Lewis *et al.* 1998) and nACh (Rovira *et al.* 1999) receptors. It is not clear whether the D→A or D→R mutation reduced single channel conductance in the 5-HT_{3A} receptor. However, inhibition of the wild-type 5-HT_{3A} receptor-mediated currents by increasing $[Ca^{2+}]_o$ from 1.8 to 10 mM was more prominent at low concentrations of 5-HT than at high concentrations. If the binding of Ca^{2+} to the D298 residue resulted in a reduced channel conductance, we would anticipate observing similar inhibition at low and high concentrations of agonist.

It is well-established that 5-HT_3 receptor function can be modulated by $[Ca^{2+}]_o$ in native neurones, neuroblastoma cells and recombinant receptor expression systems (Peters *et al.* 1988; Maricq *et al.* 1991; Gill *et al.* 1995; McMahon & Kauer, 1997; Lobitz *et al.* 2001; Niemeyer & Lummis, 2001), but little is known about the molecular determinants underlying this action of $[Ca^{2+}]_o$. We found that an increase in $[Ca^{2+}]_o$ resulted in a voltage-independent inhibition of 5-HT-activated current, which is consistent with observations from other laboratories (Peters *et al.* 1988; Gill *et al.* 1995; Niemeyer & Lummis, 2001). However, voltage-dependent inhibition of 5-HT-activated currents by $[Ca^{2+}]_o$ has also been reported (Maricq *et al.* 1991; McMahon & Kauer, 1997; van Hooft & Wadman, 2003). We demonstrated that the voltage-independent inhibition was completely eliminated by the D→A and D→R mutations, but maintained by the D→E mutation. The gating, desensitization and deactivation rates were all facilitated by increasing $[Ca^{2+}]_o$ in the wild-type receptor. Interestingly, the effects of increasing $[Ca^{2+}]_o$ on the wild-type receptor were abolished by the D→A or D→R mutations, whereas the D→E mutation maintained calcium effects similar to the wild-type receptor. Lowering $[Ca^{2+}]_o$ did not alter the function of the D298A receptor, indicating that this mutation does not result in super-sensitivity to $[Ca^{2+}]_o$, but rather appears to render the receptor insensitive to changes in this divalent cation. It is reasonable to hypothesize that Ca^{2+} modulates protein function through interactions with negatively charged amino acid side-chains (Cowan, 1996). The negatively charged ring formed by the D298 residues in the pentameric homoprotein could attract divalent ions to bind to the residues which ultimately reduce ion current. Indeed, the main contribution of D298 to 5-HT_{3A} receptor gating may be through interactions with divalent cations. Our findings provide strong evidence that the charge at D298 is responsible for the changes resulting from the D→A or D→R mutation and modulation by extracellular Ca^{2+}. $[Mg^{2+}]_o$ modulates the 5-HT_3 receptor in a similar manner to $[Ca^{2+}]_o$ (Peters *et al.* 1988; Gill *et al.* 1995; Niemeyer & Lummis, 2001), and the 20′ site of the nACh receptor has been implicated in Mg^{2+} blockade of that receptor (Imoto *et al.* 1988). We have also observed that increasing $[Mg^{2+}]_o$ accelerates activation, desensitization and deactivation kinetics of the 5-HT_{3A} receptor (X.-Q. Hu, unpublished data). It is likely that both Mg^{2+} and Ca^{2+} modulate 5-HT_{3A} receptor function via interactions involving the D298 residue.

The conformational change triggered by agonist binding is propagated from the binding sites in the extracellular domain to the channel gate. The transition between the ligand-bound closed and open states is associated with an intramolecular movement of TM2 (Unwin, 1995, 2003; Karlin, 2002). It has been suggested that the TM2–TM3 loop is involved in relaying this conformational change (Lynch *et al.* 1997; Kash *et al.* 2003; Miyazawa *et al.* 2003; Bouzat *et al.* 2004). It has been found that the TM2 half of the TM2–TM3 loop undergoes a conformational change associated with channel gating in both the glycine and $GABA_A$ receptors (Lynch *et al.* 2001; Bera *et al.* 2002). The movement of the TM2–TM3 loop could trigger the TM2 region to twist, hence opening the channel (Miyazawa *et al.* 2003; Unwin, 2003). Positioned at the border between the TM2 domain and TM2–TM3 loop, D298 is in a good position to participate in conveying the binding signal to the channel gate.

There is evidence that $[Ca^{2+}]_o$ in the synaptic cleft can change during normal synaptic activity (Pumain & Heinemann, 1985; Vassilev *et al.* 1997; Egelman & Montague, 1999; Rusakov & Fine, 2003) and in pathophysiological conditions such as epilepsy and anoxia (Lux *et al.* 1986; Brown *et al.* 1998*a*). The 5-HT_{3A} receptor is sensitive to changes in $[Ca^{2+}]_o$, although not nearly as sensitive as processes such as neurotransmitter secretion. Nonetheless, changes in calcium such as those predicted by Egelman & Montague (1999) could modulate 5-HT_{3A} receptor function in the brain during physiological and pathological changes in brain function.

In summary, our study has demonstrated that abolishing the negative charge at D298 with either the D→A/R mutations or binding of Ca^{2+} accelerated kinetics of activation, desensitization and deactivation, whereas preservation of the charge with the D→E mutation produced a receptor that resembled the wild-type receptor, exhibiting relatively slow kinetics of activation, desensitization and deactivation. Furthermore, the modulation of 5-HT_{3A} receptor function by extracellular Ca^{2+} was mimicked by the D→E mutation, and abolished by the D→A/R mutations, respectively. Our findings provide evidence supporting the role of D298 in the conformational changes involved in 5-HT_{3A} receptor gating; and reveal that the negative charge at this residue is the molecular basis of Ca^{2+} modulation of the receptor.

References

Absalom NL, Lewis TM, Kaplan W, Pierce KD & Schofield PR (2003). Role of charged residues in coupling ligand binding and channel activation in the extracellular domain of the glycine receptor. *J Biol Chem* **278**, 50151–50157.

Auerbach A & Akk G (1998). Desensitization of mouse nicotinic acetylcholine receptor channels. A two-gate mechanism. *J General Physiol* **112**, 181–197.

Bera AK, Chatav M & Akabas MH (2002). $GABA_A$ receptor M2–M3 loop secondary structure and changes in accessibility during channel gating. *J Biol Chem* **277**, 43002–43010.

Bianchi MT & Macdonald RL (2001). Agonist trapping by $GABA_A$ receptor channels. *J Neurosci* **21**, 9083–9091.

Bouzat C, Gumilar F, Spitzmaul G, Wang HL, Rayes D, Hansen SB, Taylor P & Sine SM (2004). Coupling of agonist binding to channel gating in an ACh-binding protein linked to an ion channel. *Nature* **430**, 896–900.

Brown AM, Fern R, Jarvinen JP, Kaila K & Ransom BR (1998*a*). Changes in $[Ca^{2+}]_o$ during anoxia in CNS white matter. *Neuroreport* **9**, 1997–2000.

Brown AM, Hope AG, Lambert JJ & Peters JA (1998*b*). Ion permeation and conduction in a human recombinant 5-HT_3 receptor subunit (h5-HT_{3A}). *J Physiol* **507**, 653–665.

Campos-Caro A, Sala S, Ballesta JJ, Vicente-Agullo F, Criado M & Sala F (1996). A single residue in the M2–M3 loop is a major determinant of coupling between binding and gating in neuronal nicotinic receptors. *Proc Natl Acad Sci U S A* **93**, 6118–6123.

Castaldo P, Stefanoni P, Miceli F, Coppola G, Del Giudice EM, Bellini G, Pascotto A, Trudell JR, Harrison NL, Annunziato L & Taglialatela M (2004). A novel hyperekplexia-causing mutation in the pre-transmembrane segment 1 of the human glycine receptor alpha1 subunit reduces membrane expression and impairs gating by agonists. *J Biol Chem* **279**, 25598–25604.

Ceresa BP & Limbird LE (1994). Mutation of an aspartate residue highly conserved among G-protein-coupled receptors results in nonreciprocal disruption of α_2-adrenergic receptor–G-protein interactions. *J Biol Chem* **269**, 29557–29564.

Chang Y & Weiss DS (1998). Substitutions of the highly conserved M2 leucine create spontaneously opening ρ1 γ-aminobutyric acid receptors. *Mol Pharmacol* **53**, 511–523.

Colquhoun D (1998). Binding, gating, affinity and efficacy: the interpretation of structure-activity relationships for agonists and of the effects of mutating receptors. *Br J Pharmacol* **125**, 924–947.

Cowan JA (1996). *Inorganic Biochemistry: an Introduction*, 2nd edn, ed. Wiley, New York, USA.

Davies PA, Wang W, Hales TG & Kirkness EF (2003). A novel class of ligand-gated ion channel is activated by Zn^{2+}. *J Biol Chem* **278**, 712–717.

Egelman DM & Montague PR (1999). Calcium dynamics in the extracellular space of mammalian neural tissue. *Biophys J* **76**, 1856–1867.

Gill CH, Peters JA & Lambert JJ (1995). An electrophysiological investigation of the properties of a murine recombinant 5-HT_3 receptor stably expressed in HEK 293 cells. *Br J Pharmacol* **114**, 1211–1221.

Grosman C, Salamone FN, Sine SM & Auerbach A (2000). The extracellular linker of muscle acetylcholine receptor channels is a gating control element. *J General Physiol* **116**, 327–340.

Hamill OP, Marty A, Neher E, Sakmann B & Sigworth FJ (1981). Improved patch-clamp techniques for high-resolution current recording from cells and cell-free membrane patches. *Pflugers Arch* **391**, 85–100.

Hu XQ, Zhang L, Stewart RR & Weight FF (2003). Arginine 222 in the pre-transmembrane domain 1 of 5-HT_{3A} receptors links agonist binding to channel gating. *J Biol Chem* **278**, 46583–46589.

Imoto K, Busch C, Sakmann B, Mishina M, Konno T, Nakai J, Bujo H, Mori Y, Fukuda K & Numa S (1988). Rings of negatively charged amino acids determine the acetylcholine receptor channel conductance. *Nature* **335**, 645–648.

Johnson JP Jr, Balser JR & Bennett PB (2001). A novel extracellular calcium sensing mechanism in voltage-gated potassium ion channels. *J Neurosci* **21**, 4143–4153.

Jones MV & Westbrook GL (1995). Desensitized states prolong GABAA channel responses to brief agonist pulses. *Neuron* **15**, 181–191.

Karlin A (2002). Emerging structure of the nicotinic acetylcholine receptors. *Nat Rev Neurosci* **3**, 102–114.

Kash TL, Jenkins A, Kelley JC, Trudell JR & Harrison NL (2003). Coupling of agonist binding to channel gating in the $GABA_A$ receptor. *Nature* **421**, 272–275.

Langosch D, Laube B, Rundstrom N, Schmieden V, Bormann J & Betz H (1994). Decreased agonist affinity and chloride conductance of mutant glycine receptors associated with human hereditary hyperekplexia. *EMBO J* **13**, 4223–4228.

Lewis TM, Sivilotti LG, Colquhoun D, Gardiner RM, Schoepfer R & Rees M (1998). Properties of human glycine receptors containing the hyperekplexia mutation (1 (K276E), expressed in *Xenopus* oocytes. *J Physiol* **507**, 25–40.

Lobitz N, Gisselmann G, Hatt H & Wetzel CH (2001). A single amino-acid in the TM1 domain is an important determinant of the desensitization kinetics of recombinant human and guinea pig alpha-homomeric 5-hydroxytryptamine type 3 receptors. *Mol Pharmacol* **59**, 844–851.

Lux HD, Heinemann U & Dietzel I (1986). Ionic changes and alterations in the size of the extracellular space during epileptic activity. *Adv Neurol* **44**, 619–639.

Lynch JW, Han NL, Haddrill J, Pierce KD & Schofield PR (2001). The surface accessibility of the glycine receptor M2–M3 loop is increased in the channel open state. *J Neurosci* **21**, 2589–2599.

Lynch JW, Rajendra S, Pierce KD, Handford CA, Barry PH & Schofield PR (1997). Identification of intracellular and extracellular domains mediating signal transduction in the inhibitory glycine receptor chloride channel. *EMBO J* **16**, 110–120.

McMahon LL & Kauer JA (1997). Hippocampal interneurons are excited via serotonin-gated ion channels. *J Neurophysiol* **78**, 2493–2502.

Maconochie DJ & Steinbach JH (1998). The channel opening rate of adult- and fetal-type mouse muscle nicotinic receptors activated by acetylcholine. *J Physiol* **506**, 53–72.

Maricq AV, Peterson AS, Brake AJ, Myers RM & Julius D (1991). Primary structure and functional expression of the $5HT_3$ receptor, a serotonin-gated ion channel. *Science* **254**, 432–437.

Miyazawa A, Fujiyoshi Y & Unwin N (2003). Structure and gating mechanism of the acetylcholine receptor pore. *Science* **423**, 949–955.

Niemeyer MI & Lummis SC (2001). The role of the agonist binding site in Ca^{2+} inhibition of the recombinant 5-HT_{3A} receptor. *Eur J Pharmacol* **428**, 153–161.

Ortells MO & Lunt GG (1995). Evolutionary history of the ligand-gated ion-channel superfamily of receptors. *Trends Neurosci* **18**, 121–127.

O'Shea SM & Harrison NL (2000). Arg-274 and Leu-277 of the gamma-aminobutyric acid type A receptor $\alpha 2$ subunit define agonist efficacy and potency. *J Biol Chem* **275**, 22764–22768.

Peters JA, Hales TG & Lambert JJ (1988). Divalent cations modulate 5-HT_3 receptor-induced currents in N1E-115 neuroblastoma cells. *Eur J Pharmacol* **151**, 491–495.

Pumain R & Heinemann U (1985). Stimulus- and amino acid-induced calcium and potassium changes in rat neocortex. *J Neurophysiol* **53**, 1–16.

Rajendra S, Lynch JW, Pierce KD, French CR, Barry PH & Schofield PR (1995). Mutation of an arginine residue in the human glycine receptor transforms beta-alanine and taurine from agonists into competitive antagonists. *Neuron* **14**, 169–175.

Reeves DC, Goren EN, Akabas MH & Lummis SC (2001). Structural and electrostatic properties of the 5-HT_3 receptor pore revealed by substitued cysteine accessibility mutagenesis. *J Biol Chem* **276**, 42035–42042.

Reeves DC & Lummis SC (2002). The molecular basis of the structure and function of the 5-HT_3 receptor: a model ligand-gated ion channel. *Mol Membr Biol* **19**, 11–26.

Rovira JC, Ballesta JJ, Vicente-Agullo F, Campos-Caro A, Criado M, Sala F & Sala S (1998). A residue in the middle of the M2–M3 loop of the $\beta 4$ subunit specifically affects gating of neuronal nicotinic receptors. *FEBS Lett* **433**, 89–92.

Rovira JC, Vicente-Agullo F, Campos-Caro A, Criado M, Sala F, Sala S & Ballesta JJ (1999). Gating of alpha3beta4 neuronal nicotinic receptor can be controlled by the loop M2–M3 of both $\alpha 3$ and $\beta 4$ subunits. *Pflugers Arch* **439**, 86–92.

Rusakov DA & Fine A (2003). Extracellular Ca^{2+} depletion contributes to fast activity-dependent modulation of synaptic transmission in the brain. *Neuron* **37**, 287–297.

Scheller M & Forman SA (2002). Coupled and uncoupled gating and desensitization effects by pore domain mutations in $GABA_A$ receptors. *J Neurosci* **22**, 8411–8421.

Unwin N (1995). Acetylcholine receptor channel imaged in the open state. *Nature* **373**, 37–43.

Unwin N (2003). Structure and action of the nicotinic acetylcholine receptor explored by electron microscopy. *FEBS Lett* **555**, 91–95.

van Hooft JA & Vijverberg HP (1996). Selection of distinct conformational states of the 5-HT_3 receptor by full and partial agonists. *Br J Pharmacol* **117**, 839–846.

van Hooft JA & Wadman WJ (2003). Ca^{2+} ions block and permeate serotonin 5-HT_3 receptor channels in rat hippocampal interneurons. *J Neurophysiol* **89**, 1864–1869.

Vassilev PM, Mitchel J, Vassilev M, Kanazirska M & Brown EM (1997). Assessment of frequency-dependent alterations in the level of extracellular Ca^{2+} in the synaptic cleft. *Biophys J* **72**, 2103–2116.

Watanabe J, Beck C, Kuner T, Premkumar LS & Wollmuth LP (2002). DRPEER: a motif in the extracellular vestibule conferring high Ca^{2+} flux rates in NMDA receptor channels. *J Neurosci* **22**, 10209–10216.

Zhou Q, Verdoorn TA & Lovinger DM (1998). Alcohols potentiate the function of 5-HT_3 receptor-channels on NCB-20 neuroblastoma cells by favouring and stabilizing the open channel state. *J Physiol* **507**, 335–352.

Acknowledgements

The authors thank Dr Hui Sun and Ms Amber Luo for assistance in creating the point-mutated constructs. This work was supported by the NIAAA Division of Intramural Clinical and Basic Research.